EFFECT OF TEMPERING ON THE MICROSTRUCTURE AND MECHANICAL PROPERTIES OF RESISTANCE-SPOT-WELDED DP980 DUAL-PHASE STEEL

VPLIV POPUŠČANJA NA MIKROSTRUKTURO IN MEHANSKE LASTNOSTI TOČKASTO VARJENEGA DVOFAZNEGA JEKLA DP980

Fateme Nikoosohbat[1], Shahram Kheirandish[2], Masoud Goodarzi[2], Majid Pouranvari[3]

[1]West Coast Stainless, California, USA
[2]Materials Science and Metallurgical Engineering Department, Iran University of Science and Technology (IUST), Tehran, Iran
[3]Materials and Metallurgical Engineering Department, Dezful Branch, Islamic Azad University, Dezful, Iran
mpouranvari@yahoo.com,

This paper aims at investigating the effect of an in-process tempering cycle on the microstructure and mechanical properties of the DP980 dual-phase-steel resistance spot welds. A microstructural characterization, a microhardness test and a quasi-static tensile-shear test were conducted. The results showed that the fusion-zone microstructure of as-welded spot welds mainly consisted of lath martensite. A tempered martensite region was observed in the sub-critical heat-affected zone, producing a relatively soft region compared to the base metal. It was found that applying an in-process tempering for a sufficient time promoted the heat-affected-zone softening and produced a softer fusion zone due to martensite tempering which, in turn, improved the energy-absorption capability of spot welds.

Keywords: resistance spot welding, dual-phase steel, temper, microstructure

Članek opisuje vpliv cikla popuščanja med postopkom točkastega varjenja dvofaznega jekla DP980 na mikrostrukturo in mehanske lastnosti točkastega zvara. Izvršena je bila karakterizacija mikrostrukture, izmerjena mikrotrdota in opravljen kvazi statični natezno-strižni preizkus. Rezultati so pokazali, da je mikrostruktura področja zlivanja točkastega zvara pretežno iz latastega martenzita. V območju podkritične toplotno vplivane cone je bilo opaženo področje popuščenega martenzita, ki je relativno mehko področje v primerjavi z osnovnim materialom. Ugotovljeno je bilo, da uporaba dovolj dolgega popuščanja med postopkom pospešuje mehčanje toplotno vplivane cone in nastanek mehkejše cone zlivanja zaradi popuščnega martenzita, kar hkrati izboljša zmožnost absorpcije energije točkastega zvara.

Ključne besede: uporovno točkasto varjenje, dvofazno jeklo, popuščanje, mikrostruktura

1 INTRODUCTION

Dual-phase (DP) steels exhibit a unique microstructure consisting of soft ferrite and hard martensite that offers a favorable combination of strength, high work-hardening rate, ductility and formability. Due to these features, automotive companies are finding that the use of these steels can enable them not only to reduce the overall weight of an automobile, but also providing an improved crash protection to the vehicle occupants.[1–3]

Resistance spot welding (RSW) is the main joining process of sheet metal, particularly in the automotive industry. Vehicle crashworthiness, which is defined as the capability of a car structure to provide an adequate protection to its passengers against injuries in the event of a crash, largely depends on the spot-weld structural-mechanical behavior.[4–7] Considering the development and commercialization of new DP steels for the application in automotive bodies, there is an increasing need to study the spot-welding behavior of these materials. According to the literature, the problems associated with the resistance spot welding of DP steels can be summarized as follows:[8–15]

(i) High susceptibility to failure in the interfacial failure mode

(ii) High susceptibility to expulsion

(iii) Sensitivity to the formation of shrinkage voids

(iv) High hardness of the fusion zone due to martensite formation. This can have adverse effects on the failure mode under certain loading conditions (e. g., a peel test).

Very high cooling rates in RSW cause a formation of martensite even in low-carbon steels. Tempering can then be performed by adding a post-weld current pulse (the in-process tempering step) to the welding sequence. This tempering step is a relatively simple way of reducing the weld hardness which, in turn, lowers the brittleness of the weld in C-Mn steels.[16] After the weld nugget has been formed, it is held between the electrodes long enough to sufficiently quench to martensite. A subsequent temper pulse is then applied to soften the microstructure of the weld nugget. Steels of varying composition and processing react differently to tempering and it is unknown how some of the newer transformation-hardened steels would react during such tempering.[16]

The objective of the present research is to investigate the effect of a tempering cycle on the microstructure, strength and failure energy of DP980 resistance spot welds.

2 EXPERIMENTAL PROCEDURE

A DP980-steel sheet 2 mm thick was used as the base metal. The chemical composition and mechanical properties of DP980 steel are given in **Tables 1** and **2**, respectively.

Table 1: Chemical composition of the investigated steel in mass fractions (*w*/%)
Tabela 1: Kemijska sestava preiskovanega jekla v masnih deležih (*w*/%)

P	S	Al	Cu	Cr	Si	Mn	C
0.004	0.014	0.036	0.196	0.2	0.13	1.326	0.13

Table 2: Tensile properties of the investigated DP980 steel
Tabela 2: Natezna trdnost preiskovanega jekla DP980

Yield stress (MPa)	Ultimate tensile stress (MPa)	Total elongation (%)
532	990	18

Spot welding was performed using a 120 kVA AC-pedestal-type resistance-spot-welding machine, controlled by a PLC. The welding was conducted using a 45° truncated-cone RWMA Class-2 electrode with an 8 mm face diameter. The welding and tempering were performed in accordance with the schedule given in **Table 3**.

Table 3: Welding and tempering schedule
Tabela 3: Potek varjenja in popuščanja

Squeeze time (cycle)	Welding current (kA)	Welding time (cycle)	Electrode force (kN)	Holding/Cooling time (cycle)	Tempering current (kA)	Tempering time (cycle)
40	9	35	5	40	5	20, 40

The quasi-static tensile-shear test samples were prepared according to ANSI/AWS/SAE/D8.9-97 standard.[17] **Figure 1** shows the sample dimensions used for the tensile-shear tests. The tensile-shear tests were performed at a cross head of 2 mm/min with an Instron universal
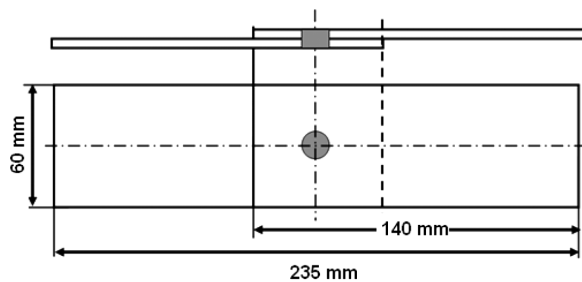
testing machine, recording the load-displacement curves. The peak load (measured as the peak point in the load-displacement curve) and the failure energy (measured as the area under the load-displacement curve up to the peak load) were extracted from the load-displacement curve.

Light microscopy was used to examine the macrostructures and to measure the weld-fusion-zone (the weld-nugget) size. The microstructures of the samples were also examined with a scanning electron microscope (SEM). The microhardness test, a technique that has proven to be useful in quantifying microstructure/mechanical property relationships, was used to determine the hardness profile parallel to the sheet interface (20 μm away from the weld centerline), using a 100 g load on a Bohler microhardness tester.

3 RESULTS AND DISCUSSION

3.1 Microstructure and hardness profile of as-welded DP980 RSWs

The microstructure and hardness profile of resistance spot welds play important roles in their failure behavior. The rapid heating and cooling induced by resistance-spot-welding thermal cycles significantly alter the microstructure in the joint zone. A typical macrostructure of a
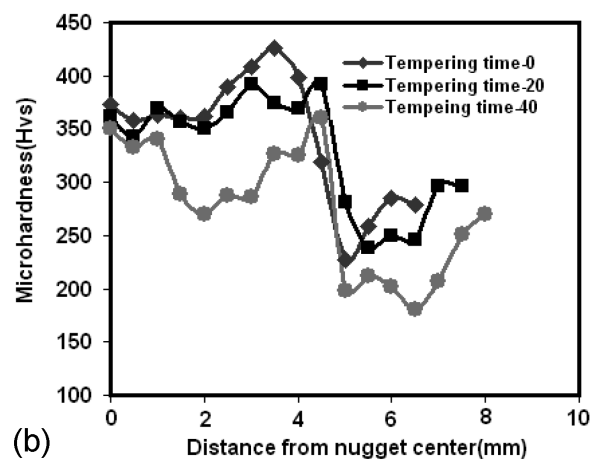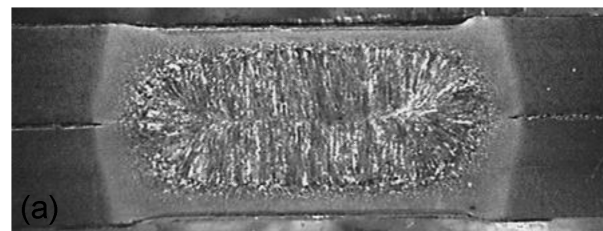

Figure 2: a) Typical macrostructure of an as-welded DP980 joint and b) hardness profile of the DP980 spot weld in the as-welded condition (i.e., tempering time = 0) and after the in-process tempering for the tempering times of 20 and 40 cycles
Slika 2: a) Značilna makrostruktura zvarjenega spoja DP980 in b) profil trdote točkastega zvara DP980 v zvarjenem stanju (čas popuščanja = 0) in po popuščanju med postopkom za čase popuščanja od 20 do 40 ciklov

Figure 1: Tensile-shear specimen dimensions
Slika 1: Dimenzije preizkušanca za natezno-strižni preizkus

DP980 spot weld is shown in **Figure 2a** indicating three distinct zones, namely, the fusion zone (FZ), the heat-affected zone (HAZ) and the base metal (BM).

The hardness profile of the DP980 RSW is shown in **Figure 2b**. The hardness variation across the joint can be analyzed in terms of the microstructure of the joint. The DP980 base-metal microstructure, as shown in **Figure 3a**, consists of dispersed martensite islands embedded in a ferrite matrix; the corresponding hardness is 300 HV (**Figure 2b**). As can be seen in **Figure 3b**, the FZ predominantly exhibits lath martensite with the average hardness of 390 HV (**Figure 2b**). The formation of a high-volume fraction of martensite in the FZ explains the higher hardness of the FZ compared to the BM hardness. The martensite formation in the FZ is attributed to the inherently high cooling rate of the resistance-spot-welding process due to the presence of water-cooled copper electrodes and their quenching effect as well as the short welding cycle. Gould et al.[18] developed a simple analytical model predicting the cooling rates of resistance spot welds. Ac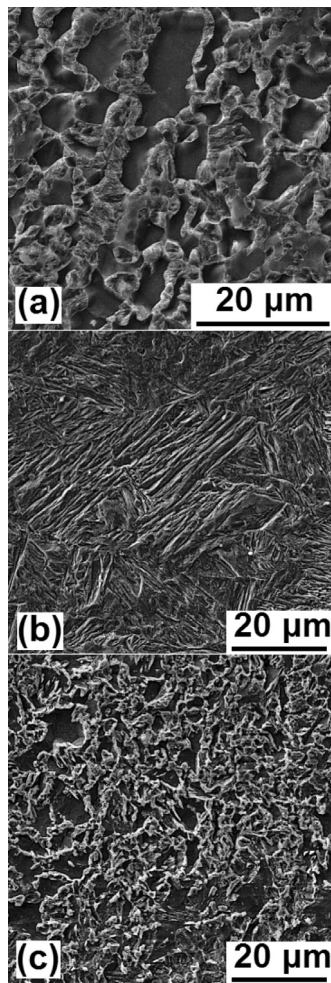cording to this model, the cooling rate for a 2 mm thickness is about 2000 K s^{-1}. For steels, the required critical cooling rate to achieve martensite in the microstructure can be estimated using the following equation:[19]

$$\lg v = 7.42 - 3.13\,w(\mathrm{C}) - 0.71\,w(\mathrm{Mn}) - 0.37\,w(\mathrm{Ni}) - 0.34\,w(\mathrm{Cr}) - 0.45\,w(\mathrm{Mo}) \qquad (1)$$

where v is the critical cooling rate (K h^{-1}).

The calculated critical cooling rate for the investigated steel is 280 K s^{-1}. Since the recorded cooling rates in the FZ are significantly higher than the critical cooling rates needed for a martensite formation, it is not surprising that a martensite structure is present in the FZ.

The hardness of the HAZ is higher than the BM hardness due to the formation of non-equilibrium phases. The microstructure of the HAZ is more heterogeneous than that of the FZ, as verified by the hardness profile. The material in the HAZ experiences the peak temperature and cooling rate, inversely proportional to its distance from the fusion line. Thus, the high-thermal cycle gradient coupled with the resulted austenite-grain structure can explain the observed microstructure gradient in the HAZ. One of the interesting features of the DP980 RSW hardness profile is the HAZ softening (i.e., the HAZ hardness reduction with respect to the BM). As can be seen, the HAZ of DP980 welds experiences an approximately 50 HV softening. The HAZ softening during the welding of DP steels was reported in[20–22]. The location of the HAZ softening corresponds to the sub-critical HAZ (i.e., the region in the HAZ that experiences the temperatures below the A_{c1} critical temperature). It is well documented that this phenomenon is due to the tempering of the pre-existing martensite in the sub-critical areas of the HAZ.[22] **Figure 3c** shows a microstructure of this region indicating a presence of the tempered martensite.

3.2 Criteria for the selection of tempering parameters

The FZ size of the spot welds made with the welding parameters from **Table 3** is about 8 mm, which is well above the conventional recommendation of 4 $t^{0.5}$ and 5 $t^{0.5}$ (t is the sheet thickness (mm)). However, the spot welds produced under the presented welding condition failed in the interfacial-failure mode. As mentioned above, it is well documented that DP steels are more prone to fail in the interfacial-failure mode. The in-process quenching and tempering of welds were used to improve the mechanical properties of the spot welds with interfacial failure.

To perform a proper quenching and tempering treatment on a weldment, the following points should be considered:

(i) The selected quenching time should be such that the weldment cools to a temperature slightly below the martensite-finish temperature (M_f) before being heated for tempering. If this temperature is above M_f, there can be untransformed austenite left in the FZ and it can re-decompose into the untempered marten-

Figure 3: SEM micrographs showing the microstructures of: a) base metal, b) fusion zone, c) HAZ softening region in the as-welded joint
Slika 3: SEM-posnetki mikrostrukture: a) osnovna kovina, b) področje zlivanja, c) HAZ-področje zmehčanja v varjenem spoju

site upon cooling to room temperature after the tempering.

(ii) In this study, to estimate the temperature distribution during the cooling cycle of spot welding, a simple analytical model predicting the cooling rates of resistance spot welds developed by Gould et al.[16,18] was used. Based on some simplification assumptions, the temperature distribution in the through-thickness direction of a steel sheet after the welding current is turned off, is expressed as follows:

$$T = T_P \frac{1 + \left(\frac{2}{\pi}\right)\left(\frac{K_E}{K_S}\right)\left(\frac{t_S}{t_E}\right)\cos\left(\frac{\pi}{2t_S}x\right)}{1 + \left(\frac{2}{\pi}\right)\left(\frac{K_E}{K_S}\right)\left(\frac{t_S}{t_E}\right)e^{\frac{\alpha\pi^2}{4t_S^2}t}} \qquad (2)$$

where T_P is the peak temperature in the spot weld, while t_S and t_E are the steel-sheet thickness and the electrode face diameter, respectively. K_S and K_E are the thermal conductivity coefficients of steel and copper, respectively. X is the distance from the weld faying surface to the electrode face, and α is the thermal diffusivity of steel.

Figure 4 shows the calculated temperature distribution for different levels of penetration in the workpiece, ranging from 0 % (the faying surface) to 100 % (the electrode-sheet surface). The temperatures in the weld at the beginning of the cooling range (0-cycle cooling in **Figure 3a**) suggest a full austenization of the weld through thickness. However, the temperatures in the extremities of the weld, approaching the electrode-sheet interfaces, are substantially cooler, being as low as 600 °C. This, of course, is well below the A_3 temperature for the material studied here, suggesting that the peripheral areas of the weld do not achieve even a partial re-austenization and, therefore, are not subjected to local martensite decomposition. Based on **Figure 4**, the quenching time between the welding cycle and the tempering cycle was selected as 40 cycles. Using a quenching time of 40
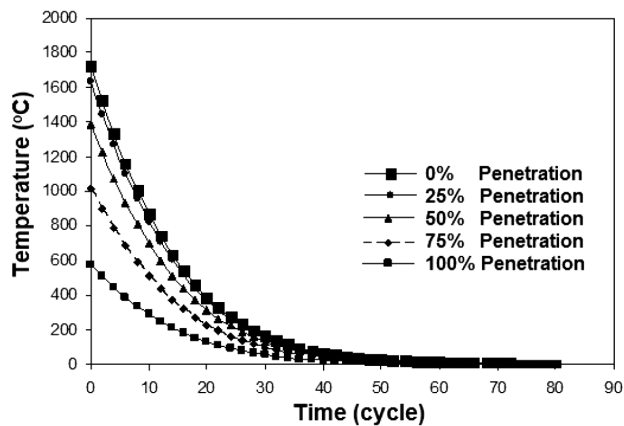

Figure 4: Calculated cooling profiles of a spot weld for different levels of penetration based on the Gould's model[16,18]
Slika 4: Profili ohlajanja točkastega zvara za različne nivoje penetracije, izračunani na osnovi Gouldovega modela[16,18]
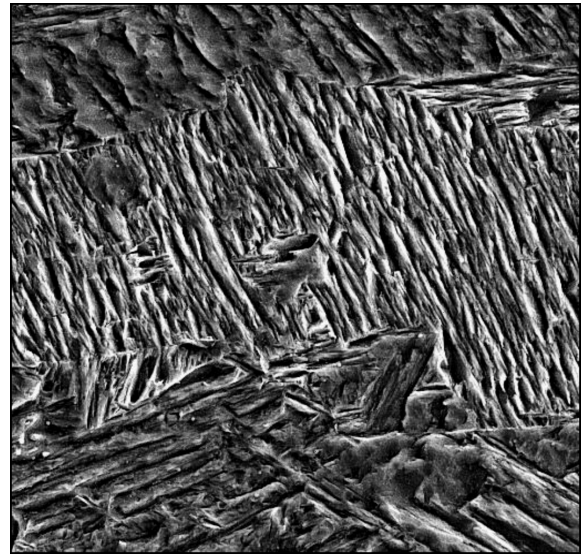

Figure 5: FZ microstructure after 20 cycles of the in-process tempering
Slika 5: Mikrostruktura področja zlivanja (FZ) po 20 ciklih popuščanja med procesom

cycles allows the weldment to cool roughly below the M_f temperature, facilitating a transformation into martensite.

3.3 Effect of the tempering cycle on the microstructure and hardness

Figure 2b shows the effect of the tempering cycle on the weld hardness. According to the hardness values of the FZ, the tempering time of 20 cycles is insufficient for the martensite to decompose. According to **Figure 5**, the FZ microstructure of the welds tempered for the tempering time of 20 cycles is still martensitic.

After a tempering time of 40 cycles a weld exhibits a relatively complex distribution of the hardness (**Figure 2b**). The macrograph of a weld after the tempering time of 40 cycles (**Figure 6a**) shows that the periphery of the weld nugget is surrounded by a narrow shell. The hardness of the weld-nugget centre is higher than that of the shell. Indeed, the weld nugget consists of an untempered fusion zone (UTFZ) and a tempered fusion zone (TFZ). This is caused by a non-uniform temperature distribution inherent during the in-situ tempering. The temperature distribution in the spot weld during the tempering is roughly parabolic in shape, with the peak temperatures always on the weld centerline.[16] Accordingly, the centre of the weld nugget can be overheated and re-austenized during the tempering cycle and, subsequently, retransformed into hard martensite during cooling, as confirmed by the high hardness of the weld center. In the shell of the TFZ, the microstructure shows evidence of tempering as shown in **Figure 6b**. Moreover, according to **Figure 2b**, the tempering cycle resulted in a softer HAZ due to a longer time of tempering the martensite present in the initial microstructure of the BM.
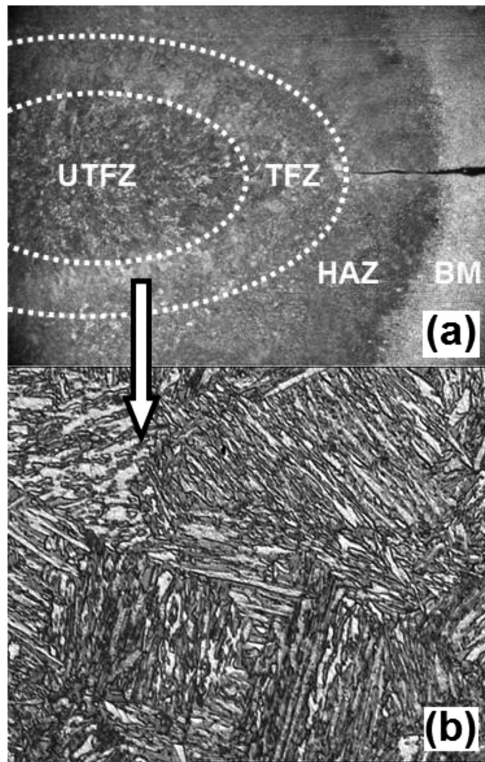
Figure 6: a) Weld-nugget macrograph after 40-cycle in-process tempering showing tempered fusion zone (TFZ) and untempered fusion zone (UTFZ), b) tempered martensite in the TFZ
Slika 6: a) Posnetek makrostrukture jedra zvara po 40 ciklih popuščanja kaže popuščeno področje zlivanja (TFZ) in nepopuščeno področje zlivanja (UTFZ), b) popuščeni martenzit v TFZ

3.4 Effect of the tempering cycle on the mechanical properties

The peak load of the spot welds depends on several factors including the physical weld attributes (mainly the FZ size and the indentation depth), the failure mode and the strength of the failure location. The failure energy of spot welds, measured as the area under the load-displacement curve up to the peak point, can be expressed as follows:

$$Energy\,absorption = \int_{0}^{l_{max}} Fdl \propto P_{max} \times l_{max} \qquad (3)$$

where P_{max} is the peak load and l_{max} is the maximum displacement, corresponding to the peak load. The maximum displacement (l_{max}) that represents the ductility of the spot welds depends on the ductility of the failure location. Therefore, the energy absorption depends on the factors governing the peak load and the ductility of the failure location.

Figure 7a shows the tensile-shear peak loads of the welds indicating that the as-welded joint (the untempered condition) exhibits the highest peak load. This can be related to the tensile-shear test configuration, which tends to load the welds in shear. Under the shear loading,
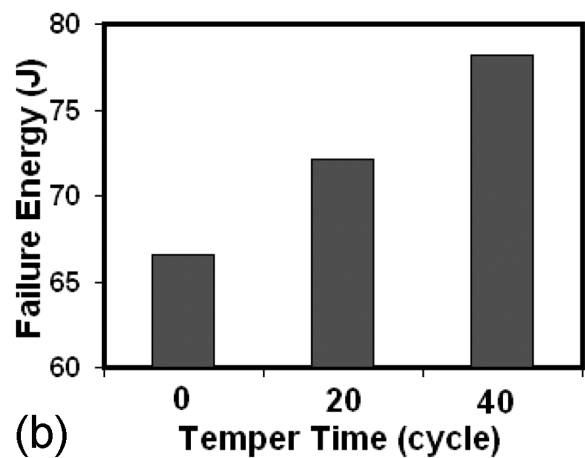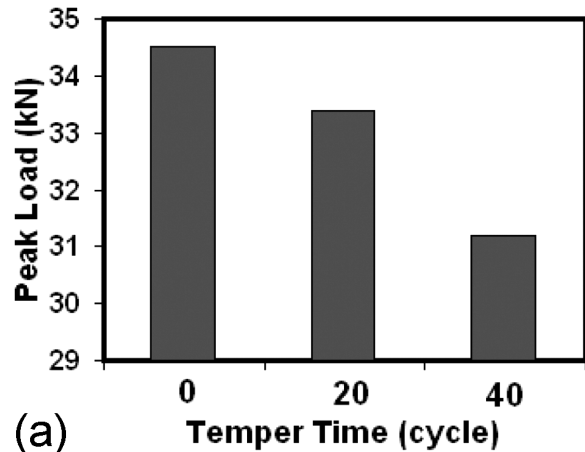

Figure 7: Effect of the tempering cycle on the weld strength and energy
Slika 7: Vpliv cikla popuščanja na trdnost in energijo zvara

any tendency for brittle fracture is minimized.[23] Therefore, the shear strength of the spot welds failed in the IF mode during the tensile-shear test depends on the strength/hardness correlation of the FZ. In the as-welded joint, the fully martensitic microstructure provides the highest peak load. The tempering which softens the FZ microstructure leads to a reduction in the strength of the joints.

Figure 7b shows the failure energy of the welds indicating a positive influence of the tempering cycle on the failure energy of the welds. According to **Figure 7b**, applying a tempering time of 40 cycles improved the weld failure energy. This can be related to the improved ductility of the FZ due to the tempering of the as-welded martensite which, in turn, enhances the energy-absorption capability of the weld. It was shown that there is a direct relationship between the failure energy in the static tensile-shear test and the impact tensile-shear test.[24] Therefore, it can be concluded that the tempering of spot welds that improves the weld energy-absorption capability increases the weld performance reliability against the impact loads such as crash accidents of cars.

4 CONCLUSIONS

1. The FZ of the as-welded spot weld exhibited a lath martensite microstructure. A reduction in the hardness (softening) with respect to the BM was observed in the HAZ due to the tempering of the martensite present in the initial microstructure of the base metal.

2. A short tempering cycle (i.e., a tempering time of 20 cycles) was insufficient for the lamellar martensite microstructure in the FZ to decompose. With the increasing tempering time, the martensite tempering in the FZ increased, resulting in a reduction of the average hardness of the FZ compared with that of the as-welded condition. Moreover, applying a tempering cycle led to an enlargement of the HAZ softening region.

3. It was shown that applying the in-process tempering for a sufficient time generates a pronounced HAZ softening and a softer fusion zone due to martensite tempering that, in turn, improves the energy-absorption capability of the welds.

5 REFERENCES

[1] M. Pouranvari, Influence of welding parameters on peak load and energy absorption of dissimilar resistance spot welds of DP600 and AISI1008 steels, Can Metall Q, 50 (**2001**), 381–88

[2] P. Movahed, S. Kolahgar, S. P. H. Marashi, M. Pouranvari, N. Parvin, The effect of intercritical heat treatment temperature on the tensile properties and work hardening behavior of ferrite–martensite dual phase steel sheets, Mater Sci Eng A, 518 (**2009**), 1–6

[3] M. Delincea, Y. Brechet, J. D. Emburyc, M. G. D. Geersd, P. J. Jacquesa, T. Pardoena, Separation of size-dependent strengthening contributions in fine-grained dual phase steels by nanoindentation, Acta Mater, 55 (**2007**), 2337–50

[4] M. Pouranvari, E. Ranjbarnoodeh, Dependence of the fracture mode on the welding variables in the resistance spot welding of ferrite-martensite DP980 advanced high-strength steel, Mater. Tehnol., 46 (**2012**) 6, 665–671

[5] P. Podrzaj, S. Simoncic, Resistance spot welding control based on fuzzy logic, Int J Adv Manuf Technol., 52 (**2011**), 959–967

[6] P. Podrzaj, S. Simoncic, Resistance spot welding control based on the temperature measurement, Sci Technol Weld Join, 18 (**2013**), 551–557

[7] M. Pouranvari, S. M. Mousavizadeh, Failure Mode of M130 Martensitic Steel Resistance-Spot Welds, Mater. Tehnol., 47 (**2013**) 6, 771–776

[8] M. Pouranvari, S. P. H. Marashi, Critical review of automotive steels spot welding: process, structure and properties, Sci Technol Weld Join, 18 (**2013**), 361–403

[9] M. M. H. Abadi, M. Pouranvari, Failure-mode transition in resistance spot welded DP780 advanced high-strength steel: effect of loading conditions, Mater. Tehnol., 48 (**2014**) 1, 67–71

[10] M. Pouranvari, S. P. H. Marashi, D. S. Safanama, Failure mode transition in AHSS resistance spot welds, Part II: Experimental investigation and model validation, Mater Sci Eng A, 528 (**2011**), 8344–52

[11] M. Pouranvari, H. R. Asgari, S. M. Mosavizadeh, P. H. Marashi, M. Goodarzi, Effect of weld nugget size on overload failure mode of resistance spot welds, Sci Technol Weld Join, 12 (**2007**), 217–25

[12] M. Pouranvari, S. P. H. Marashi, Failure mode transition in AHSS resistance spot welds, Part I, Controlling factors, Mater Sci Eng A, 528 (**2011**), 8337–43

[13] M. Pouranvari, Failure mode transition in similar and dissimilar resistance spot welds of HSLA and low carbon steels, Can Metall Q, 51 (**2012**), 67–74

[14] S. Simoncic, P. Podrzaj, Image-based electrode tip displacement in resistance spot welding, Meas Sci Technol, 23 (**2012**) 6, 065401

[15] X. Sun, E. V. Stephens, M. A. Khaleel, Effects of fusion zone size and failure mode on peak load and energy absorption of advanced high strength steel spot welds under lap shear loading conditions, Eng Fail Anal, 15 (**2008**), 356–67

[16] W. Chuko, J. Gould, Development of Appropriate Resistance Spot Welding Practice for Transformation-Hardened Steels, Report to the American Iron and Steel Institute, 2002

[17] Recommended Practices for Test Methods and Evaluation the Resistance Spot Welding Behavior of Automotive Sheet Steels, ANSI/AWS/SAE D8.9–97, 1997

[18] J. E. Gould, S. P. Khurana, T. Li, Predictions of microstructures when welding automotive advanced high-strength steels, Weld J, 86 (**2006**), 111–6

[19] K. E. Easterling, Modelling the weld thermal cycle and transformation behavior in the heat-affected zone, In: H. Cerjak, K. E. Easterling (Eds.), Mathematical Modelling of Weld Phenomena, 1st ed., Maney Publishing, 1993

[20] F. Nikoosohbat, S. Kheirandish, M. Goodarzi, M. Pouranvari, S. P. H. Marashi, Microstructure and failure behaviour of resistance spot welded DP980 dual phase steel, Mater Sci Technol, 26 (**2010**), 738–44

[21] M. Pouranvari, S. P. H. Marashi, Key factors influencing mechanical performance of dual phase steel resistance spot welds, Sci Technol Weld Join, 15 (**2010**), 149–155

[22] V. H. B. Hernandez, S. K. Panda, M. L. Kuntz, Y. Zhou, Nanoindentation and microstructure analysis of resistance spot welded dual phase steel, Mater Lett, 64 (**2010**), 207–210

[23] R. W. Hertzberg, Deformation and fracture mechanics of engineering materials, 2nd ed, John Wiley & Sons, 1996

[24] M. Zhou, H. Zhang, S. J. Hu, Critical Specimen Sizes for Tensile-Shear Testing of Steel Sheets, Weld J, 78 (**1999**), 305–313